PHYSICAL REVIEW D **80,** 092002 (2009)

Prospects for the measurement of the unitarity triangle angle γ from $B^0 \to DK^+\pi^-$ decays

Tim Gershon[1] and Mike Williams[2]

[1]*Department of Physics, University of Warwick, Coventry CV4 7AL, United Kingdom*
[2]*Physics Department, Imperial College London, London SW7 2AZ, United Kingdom*

(Received 18 September 2009; published 5 November 2009)

The potential for a precise measurement of the unitarity triangle angle γ in future experiments from the decay $B^0 \to DK^{*0}$ is well known. It has recently been suggested that the sensitivity can be significantly enhanced by analyzing the $B^0 \to DK^+\pi^-$ Dalitz plot to extract amplitudes relative to those of the flavor-specific decay $B^0 \to D_2^{*-}K^+$. An extension to this method which includes the case where the neutral D meson is reconstructed in suppressed final states is presented. The sensitivity to γ is estimated using this method and compared to that obtained using the $B^0 \to DK^{*0}$ decay alone. Experimental effects, such as background contamination, are also considered. This approach appears to be a highly attractive addition to the family of methods that can be used to determine γ.

DOI: 10.1103/PhysRevD.80.092002 PACS numbers: 13.25.Hw, 12.15.Hh, 11.30.Er

I. INTRODUCTION

The quark flavor sector of the standard model of particle physics, described by the Cabibbo-Kobayashi-Maskawa (CKM) quark mixing matrix [1,2], gives a successful description of all current experimental measurements of quark flavor-changing interactions. It also provides an excellent laboratory to search for effects of physics beyond the standard model (see, for example, Refs. [3–5]). A critical element of this program is the precise measurement of the angle $\gamma = \arg(-V_{ud}V_{ub}^*/V_{cd}V_{cb}^*)$ of the unitarity triangle formed from elements of the CKM matrix.

A method to measure γ with negligible theoretical uncertainty was proposed by Gronau, London, and Wyler (GLW) [6,7]. The original method uses $B \to DK$ decays, with the neutral D meson reconstructed in CP eigenstates. The method can be extended to use D meson decays to any final state that is accessible to both D^0 and $\bar{D}^0$, in particular, doubly Cabibbo-suppressed decays such as $K^+\pi^-$ [8,9] have been noted to provide enhanced sensitivity to CP-violation effects.

The use of neutral B decays is particularly interesting since the two contributing amplitudes are more similar in magnitude, so that direct CP-violation effects may be enhanced relative to those in charged B decays. The decay $B^0 \to DK^{*0}$ is especially advantageous since the charge of the kaon in the $K^{*0} \to K^+\pi^-$ decay unambiguously tags the flavor of the decaying B meson, obviating the need for time-dependent analysis [10]. This appears to be one of the most promising channels for LHCb to make a precise measurement of γ [11–13].

The approach that has mainly been considered until recently is a quasi-two-body analysis of $B^0 \to DK^{*0}$. In this analysis, the contributions from other resonances in the $B^0 \to DK^+\pi^-$ Dalitz plot that interfere with the K^{*0} within the selected mass window are handled by the introduction of an additional hadronic parameter [14]. This parameter, normally denoted by κ, takes values between 0 and 1 where 0 implies that all sensitivity to γ is lost, and the limit of 1 is reached in the case that no amplitudes other than DK^{*0} contribute. Estimates suggest that $0.9 < \kappa < 1.0$ for a K^{*0} mass window of ± 50 MeV [15].

Recently it has been noted that the natural width of the K^* meson can be used to enhance the sensitivity to the CP-violating phase γ through analysis of the $B^0 \to DK^+\pi^-$ Dalitz plots [16,17]. By comparison of the Dalitz-plot distributions of events in the cases where the neutral D meson is reconstructed in flavor-specific and CP-eigenstate modes, the complex amplitudes of the DK^{*0} decays can each be determined relative to the flavor-specific $D_2^{*-}K^+$ amplitude. This allows for a direct extraction of γ from the difference in amplitudes, rather than from the rates.

In this paper we extend the method proposed in Ref. [17] to include also the case where the neutral D meson is reconstructed in suppressed final states. This allows us to make a direct comparison of the sensitivity to γ between the quasi-two-body analysis and the Dalitz-plot analysis. We also study possible systematic effects that may limit the sensitivity of the analysis, including uncertainties on the correct composition of the Dalitz-plot model and a brief discussion of experimental effects.

The remainder of the paper is organized as follows: in Sec. II we give an overview of the method; in Sec. III we describe the Dalitz-plot model used for our study; in Secs. IV and V we present the results we obtain in the quasi-two-body analysis and in the Dalitz-plot analysis, respectively; in Sec. VI we discuss how experimental effects can be handled, before summarizing in Sec. VII.

II. METHOD

In this section we describe the various methods that can be used to extract γ from $B \to DK^{(*)}$. We first review the quasi-two-body approach, and then recap the recently proposed Dalitz-plot technique [17], before describing the

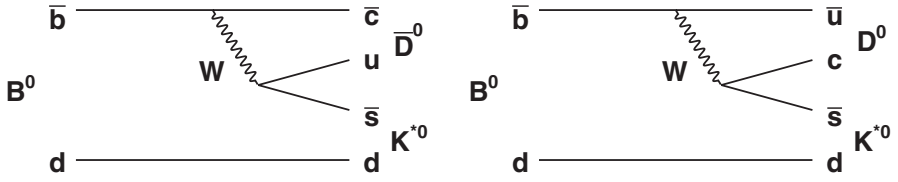

FIG. 1. Feynman diagrams for $B^0 \to DK^{*0}$, via (left) a $\bar{b} \to \bar{c}u\bar{s}$ transition and (right) a $\bar{b} \to \bar{u}c\bar{s}$ transition.

extension to the method used in our study. All methods exploit the interference between the two tree-level amplitudes shown in Fig. 1. Conventionally, the ratio of magnitudes of these two amplitudes is referred to as r_B, while their strong phase difference is labeled δ_B.

The GLW method [6,7] of extracting γ uses the following rates and asymmetries in $B \to DK^{(*)}$ decays:

$$R_\pm = \frac{\Gamma(\bar{B} \to D_\pm \bar{K}^{(*)}) + \Gamma(B \to D_\pm K^{(*)})}{\Gamma(\bar{B} \to D_{\rm fav} \bar{K}^{(*)}) + \Gamma(B \to D_{\rm fav} K^{(*)})} = 1 + r_B^2 \pm 2r_B \cos(\delta_B)\cos(\gamma), \quad (1)$$

$$A_\pm = \frac{\Gamma(\bar{B} \to D_\pm \bar{K}^{(*)}) - \Gamma(B \to D_\pm K^{(*)})}{\Gamma(\bar{B} \to D_\pm \bar{K}^{(*)}) + \Gamma(B \to D_\pm K^{(*)})} = \frac{\pm 2r_B \sin(\delta_B)\sin(\gamma)}{R_\pm}. \quad (2)$$

Here, $\bar{B}$ (B) is used to refer to either B^- or $\bar{B}^0$ (B^+ or B^0), while $D_\pm$ refers to a neutral D meson reconstructed in a CP-even (e.g. K^+K^-) or CP-odd (e.g. $K^0_S\pi^0$) final state, and $D_{\rm fav}$ refers to a neutral D meson reconstructed in a favored, quasi-flavor-specific (e.g. $D^0 \to K^-\pi^+$) final state. Note that experimentally it is convenient to measure $R_\pm$ normalized to an equivalent double ratio from $B \to D\pi$ or $B \to D\rho$ decays.

Since $R_+A_+ + R_-A_- = 0$, the above four observables give three independent constraints on the three parameters γ, r_B, and δ_B. This is sufficient to solve the system up to an eightfold ambiguity. However, when measurements are performed in a hadronic environment as at LHCb, the reconstruction of the CP-odd final states becomes a significant experimental problem. Therefore, additional observables are required.

A solution is to include doubly Cabibbo-suppressed D meson decays, as first suggested by Atwood, Dunietz, and Soni (ADS) [8,9]. Because of the fact that the D meson decays to $K^\pm\pi^\mp$ are not truly flavor specific, but include a suppressed contribution which is given by $r_D e^{i\delta_D}$ relative to the favored decay amplitude,[1] enhanced CP-violation effects can occur. The rates and asymmetries of the $B \to DK^{(*)}$ decays to the suppressed final states are then given by

$$R_{\rm ADS} = \frac{\Gamma(\bar{B} \to D_{\rm sup}\bar{K}^{(*)}) + \Gamma(B \to D_{\rm sup}K^{(*)})}{\Gamma(\bar{B} \to D_{\rm fav}\bar{K}^{(*)}) + \Gamma(B \to D_{\rm fav}K^{(*)})} = r_B^2 + r_D^2 + 2r_B r_D \cos(\delta_B - \delta_D)\cos(\gamma), \quad (3)$$

$$A_{\rm ADS} = \frac{\Gamma(\bar{B} \to D_{\rm sup}\bar{K}^{(*)}) - \Gamma(B \to D_{\rm sup}K^{(*)})}{\Gamma(\bar{B} \to D_{\rm sup}\bar{K}^{(*)}) + \Gamma(B \to D_{\rm sup}K^{(*)})} = \frac{2r_B r_D \sin(\delta_B - \delta_D)\sin(\gamma)}{R_{\rm ADS}}. \quad (4)$$

Since the hadronic parameters of the D decay (r_D and δ_D) can be determined independently [18,19], these measurements provide two additional linearly independent constraints that can be used in combination with the GLW observables to obtain bounds on the three unknown parameters γ, r_B, and δ_B. With the decay modes $D \to K^\pm\pi^\mp$, the ADS observables are well suited to reconstruction in a hadronic environment. Consequently, one of the most promising strategies for the tree-level determination of γ at LHCb is that from the combination of measurements of R_+, A_+, $R_{\rm ADS}$, and $A_{\rm ADS}$ in charged $B \to DK$ decays [20] or neutral $B \to DK^*$ decays [11,13].

The finite width of the $K^{*0}(892)$ resonance leads to additional complications in the analysis of $B \to DK^*$ decays, since other contributions to the $B \to DK\pi$ Dalitz plot can affect the population within the K^* mass window. This can be handled by making the following substitutions [14]:

$$r_B \to r_S = \sqrt{\frac{\int_{\rm DP} |A_u|^2 d\vec{x}}{\int_{\rm DP} |A_c|^2 d\vec{x}}}, \quad (5)$$

$$e^{i\delta_B} \to \kappa e^{i\delta_S} = \frac{\int_{\rm DP} |A_u||A_c| e^{i\delta} d\vec{x}}{\sqrt{\int_{\rm DP} |A_u|^2 d\vec{x} \int_{\rm DP} |A_c|^2 d\vec{x}}}, \quad (6)$$

where A_c and A_u are, respectively, the amplitudes carrying the phase of the $\bar{b} \to \bar{c}u\bar{s}$ [Fig. 1(left)] and of the $\bar{b} \to \bar{u}c\bar{s}$ [Fig. 1(right)] transitions, and δ is the strong phase difference between them, all as functions of the Dalitz-plot position $\vec{x}$. The integrals are over the region of the Dalitz plot that is defined as the K^* mass window. In the limit that DK^* is the only contribution in this window, $r_S \to r_B$, $\delta_S \to \delta_B$, and $\kappa \to 1$.

With this treatment, the two hadronic parameters associated with the DK^* decay (r_B and δ_B) are replaced with two effective parameters (r_S and δ_S) and a new unknown (κ) is introduced. Since the combination of (CP-even)

[1]Note that the sign convention for δ_D used in this paper is opposite to that used in most of the literature on γ measurements.

GLW and ADS observables provides four linearly independent measurements, it is possible to determine κ from the data together with γ, r_B, and δ_B. Alternatively, external input, either theoretical or experimental, could be used to constrain κ [15].

We refer to the extraction of γ using the approach outlined above as the quasi-two-body analysis. The addition of ADS observables helps one to resolve two of the ambiguities of the GLW approach [21]; however, the effectiveness of this depends on the values of r_D, δ_D, and δ_B, as well as the statistical sensitivity. Moreover, the sensitivity to γ depends on the values of the unknown hadronic parameters, particularly δ_B.

The recently proposed $B \to DK\pi$ Dalitz-plot analysis [17] exploits the presence of the $B \to D_2^* K$ contribution that serves as a reference amplitude, since the flavor of the neutral D meson produced in $D_2^{*\pm} \to D\pi^\pm$ is tagged by the charge of the accompanying pion. Considering flavor-specific D mesons, we can define the $B \to DK^*$ amplitude relative to this reference, as illustrated in Fig. 2 (left),

$$\frac{A(B^0 \to \bar{D}^0 K^{*0})}{A(B^0 \to D_2^{*-} K^+)} = \varrho e^{i\Delta}. \tag{7}$$

Note that in Eq. (7) and throughout the discussion below, we neglect factors of $A(K^{*0} \to K^+\pi^-)$ and $A(D_2^{*-} \to \bar{D}^0\pi^-)$ that formally should appear in the numerator and denominator, respectively, since they eventually cancel in the observables of interest.

Considering now CP-even D mesons, using the convention $D_\pm = \frac{1}{\sqrt{2}}(D^0 \pm \bar{D}^0)$, we find [see Fig. 2(right)]

$$\frac{\sqrt{2}A(B^0 \to D_+ K^{*0})}{\sqrt{2}A(B^0 \to D_{2+}^{*-} K^+)} = \varrho e^{i\Delta}(1 + r_B e^{i(\delta_B+\gamma)}), \tag{8}$$

where D_{2+}^{*-} denotes that the neutral D meson produced in the decay of the D_2^{*-} is reconstructed in a CP-even eigenstate. Thus, we find [17]

$$\begin{aligned} x_+ + iy_+ &= r_B e^{i(\delta_B+\gamma)} \\ &= \frac{(\sqrt{2}A(D_+ K^{*0}))/(\sqrt{2}A(D_{2+}^{*-} K^+))}{(A(\bar{D}^0 K^{*0}))/(A(D_2^{*-} K^+))} - 1 \\ &= \frac{\sqrt{2}A(D_+ K^{*0})}{A(\bar{D}^0 K^{*0})} - 1, \end{aligned} \tag{9}$$

where the variables (x_+, y_+) are the same as those used in the analysis of $B \to DK$ with $D \to K_S^0\pi^+\pi^-$ decays [22,23]. Constraints on $x_- + iy_- = r_B e^{i(\delta_B-\gamma)}$ are likewise obtained from equivalent expressions for the charge-conjugate $\bar{B}^0$ decays. The extraction of γ from this Dalitz-plot analysis with only a single unresolvable ambiguity ($\gamma \to \gamma + \pi$, $\delta_B \to \delta_B + \pi$) is possible using only CP-even D decays. Consequently, we restrict our discussion to CP-even D decays, since those are experimentally accessible in a hadronic environment; however, we note that CP-odd decays give similar expressions, but with the right-hand side of the last two relations of Eq. (9) multiplied by a minus sign.

The discussion above, and in Ref. [17], considers that the D mesons used for normalization are reconstructed in flavor-specific final states. However, as already mentioned, the favored decay $D^0 \to K^-\pi^+$ is only approximately flavor specific. Furthermore, since the doubly Cabibbo-suppressed decays are used to great benefit in the quasi-

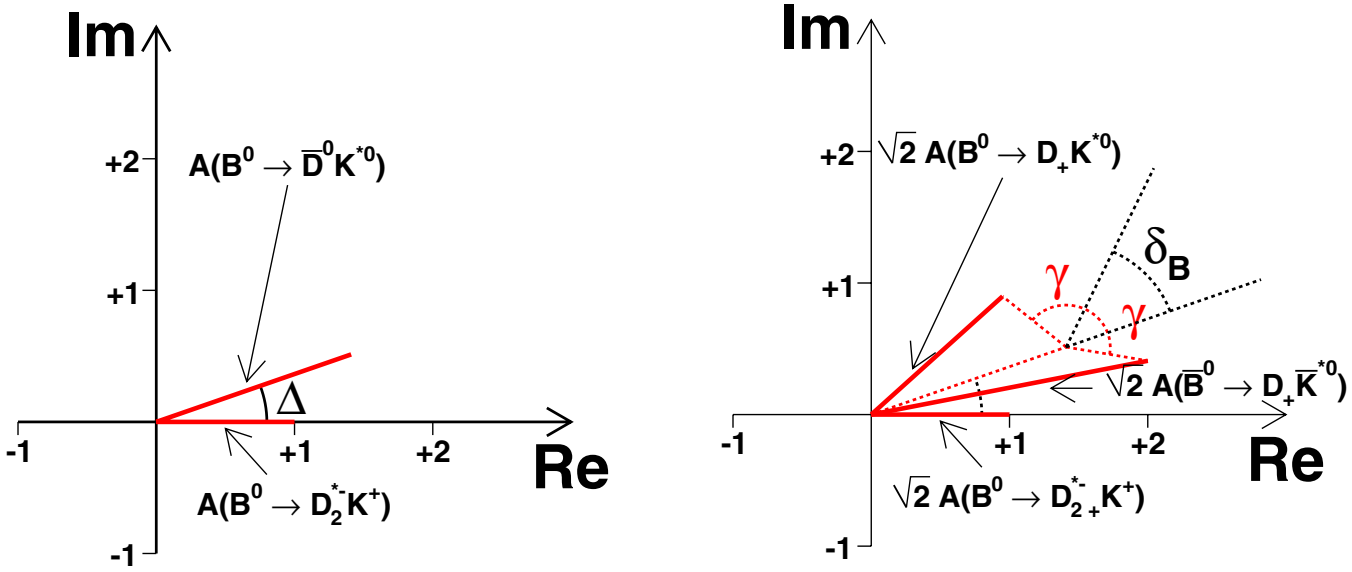

FIG. 2 (color online). Argand diagrams illustrating the measurements of relative amplitudes and phases from analysis of the Dalitz plots of (left) $\bar{D}^0 K^+\pi^-$ and (right) $D_{CP}K^+\pi^-$. In these illustrative examples the following values are used: $\varrho = 1.5$, $\Delta = 20°$, $\gamma = 75°$, $\delta_B = 45°$, and $r_B = 0.4$.

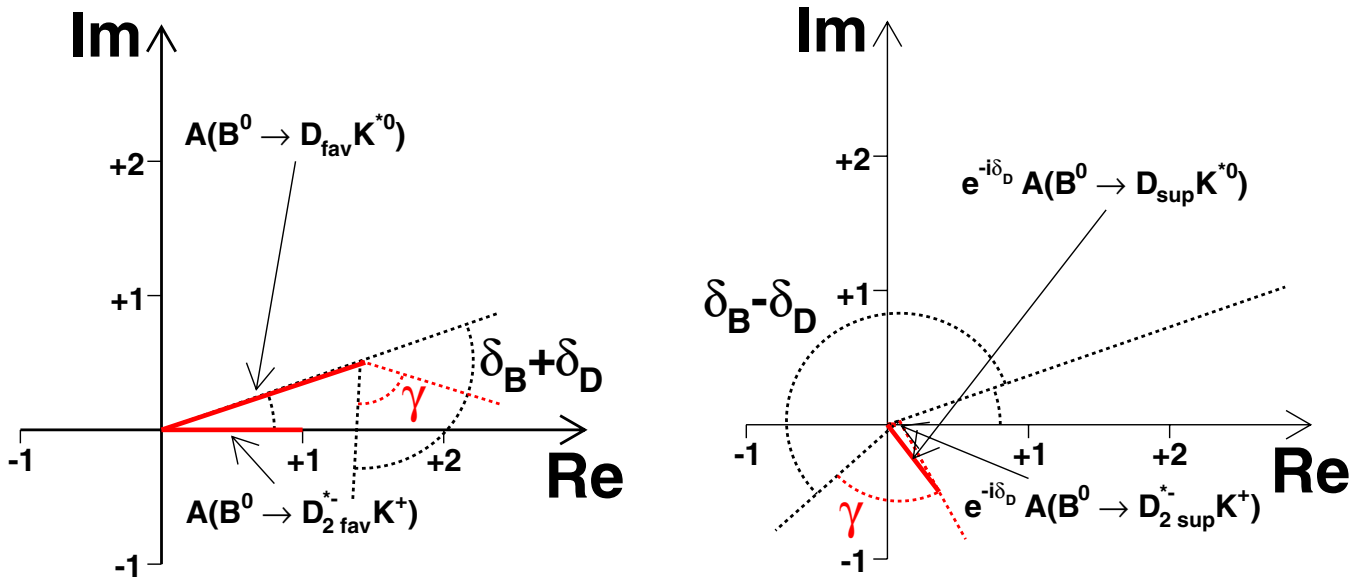

FIG. 3 (color online). Argand diagrams illustrating the measurements of relative amplitudes and phases from analysis of the Dalitz plots of (left) $D_{\rm fav}K^+\pi^-$ and (right) $D_{\rm sup}K^+\pi^-$. Note that in the latter the amplitudes are rotated by $-\delta_D$ to maintain the convention of having the $D_2^{*-}K^+$ amplitude on the real axis. In these illustrative examples the following values are used: $\varrho = 1.5$, $\Delta = 20°$, $\gamma = 75°$, $\delta_B = 45°$, $r_B = 0.4$, $\delta_D = -158°$, and $r_D = 0.06$.

two-body analysis, it is reasonable to ask if they can also be included in the Dalitz-plot analysis. We therefore extend the method to include the effects of the suppressed D-decay amplitudes. We find

$$\frac{A(B^0 \to D_{\rm fav}K^{*0})}{A(B^0 \to D^{*-}_{2\,\rm fav}K^+)} = \varrho e^{i\Delta}(1 + r_B r_D e^{i(\delta_B+\delta_D+\gamma)}), \quad (10)$$

$$\frac{A(B^0 \to D_{\rm sup}K^{*0})}{A(B^0 \to D^{*-}_{2\,\rm sup}K^+)} = \varrho e^{i\Delta}\left(1 + \frac{r_B}{r_D}\, e^{i(\delta_B-\delta_D+\gamma)}\right), \quad (11)$$

while the expression for the amplitude ratio in the Dalitz plot with the CP-even D meson is unchanged from Eq. (8). These amplitudes are illustrated in Fig. 3. As before, the equivalent expressions for the charge-conjugate $\bar{B}^0$ decays are obtained with the substitution $\gamma \to -\gamma$.

As one would expect, the amplitudes obtained from the $D_{\rm fav}K^+\pi^-$ Dalitz plot [Fig. 3(left)] are hardly distinguishable from those for the idealized flavor-specific D decays. As discussed in Ref. [17], if the suppressed amplitudes are neglected, it will lead to only a small bias in the extraction of γ.

The amplitudes obtained from the $D_{\rm sup}K^+\pi^-$ Dalitz plot [Fig. 3(right)] are markedly different from those of the other Dalitz plots, and this new information can in principle be used to constrain γ. However, in this case the D_2^*K contribution is no longer suitable as a reference amplitude, due to its small size, and the measurement of the relative phase between D_2^*K and DK^* amplitudes would be expected to have a large uncertainty. Nonetheless, it should be possible to obtain information about the relative magnitude of these amplitudes, which will provide sensitivity to γ. Note that, in contrast to the quasi-two-body analysis, it is not necessary to use external constraints on r_D and δ_D in the Dalitz-plot analysis.

III. $B \to DK\pi$ DALITZ-PLOT MODEL

We construct a model for $B \to DK\pi$ Dalitz-plot distributions using the isobar formalism, in which the total amplitude is written as the coherent sum of contributions from resonant and nonresonant terms:

$$\mathcal{M}(\vec{x}) = a_{\rm nr}e^{i\phi_{\rm nr}} + \sum_r a_r e^{i\phi_r} F_{B\to Rb(\vec{x})} F_{R\to d_1 d_2(\vec{x})} \times BW_r(\vec{x}) S_r(\vec{x}). \quad (12)$$

In Eq. (12), $\vec{x} = (m^2_{K\pi}, m^2_{D\pi})$ represents the position in the Dalitz plot, $ae^{i\phi}$ describes the complex amplitude for each component, the F terms denote vertex form factors, BW the resonance propagator and S the Lorentz invariant spin factor. We use Blatt-Weisskopf barrier form factors [24], and use relativistic Breit-Wigner line shapes to describe the propagators. We use the Zemach formalism [25,26] for the spin factors. We assume that the nonresonant contribution is constant across the phase space. This is a sufficient approximation for the study at hand, even though a more complicated description is likely to be necessary to fit real data. All amplitudes are evaluated using the `qft++` package [27].

We develop a model for the $B^0 \to DK^+\pi^-$ Dalitz-plot distribution based on the following results from Ref. [28]:

$$\mathcal{B}(B^0 \to DK^+\pi^-) = (88 \pm 15 \pm 9) \times 10^{-6},$$
$$\mathcal{B}(B^0 \to DK^{*0}(892)[K^+\pi^-]) = (38 \pm 6 \pm 4) \times 10^{-6},$$
$$\mathcal{B}(B^0 \to D_2^{*-}(2460)[D\pi^-]K^+) = (18.3 \pm 4.0 \pm 3.1) \times 10^{-6},$$
$$\mathcal{B}(B^0 \to DK^+\pi^-)_{\rm nr} = (26 \pm 8 \pm 4) \times 10^{-6}.$$

The results for the resonant contributions were extracted using events in the regions $|M_{K\pi} - M_{K^{*0}}| < 150$ MeV and $|M_{D\pi} - M_{D_2^{*-}}| < 75$ MeV, respectively. The strengths of the $K^*(892)$ and $D_2^{*-}(2460)$ amplitudes in our model were set by requiring that the fit fractions of these resonances in these regions match the published results [28].

Since we expect the Dalitz plot to contain contributions from other resonances not considered in Ref. [28], we add additional contributions based on results from an analysis of the $B^0 \to D^{\pm}K_S^0\pi^{\mp}$ Dalitz plot [29], taking isospin and color-suppression factors into account as appropriate. Some additional scaling of these resonance terms was performed to provide a better match to the results published in Ref. [28]. These experimental results provide information about the likely magnitude of contributions from K^* and D^* resonances to the Dalitz plot.

Additionally, contributions from D_s^*-type resonances can in principle contribute. Their effect could be significant since they are mediated by $b \to u$ transitions which provide the sensitivity to γ. The $D_{s2}^*(2573)$ and $D_{s1}^*(2700)$ states are known to decay to DK, and the latter has been observed in B decays [30]. These are not included in our nominal model, but we consider their potential effect among the model variations discussed below in Sec. V.

TABLE I. Parameters of resonances used in the model [31].

Resonance	J^P	Mass (MeV)	Width (MeV)
$K^*(892)$	1^-	896	51
$K_0^*(1430)$	0^+	1412	294
$K_2^*(1430)$	2^+	1432	109
$K^*(1680)$	1^-	1717	322
$D_0^*(2400)$	0^+	2403	283
$D_2^*(2460)$	2^+	2459	25
$D_{s1}^*(2700)$	1^-	2690	110

TABLE II. Summary of the $B \to D_{\rm fav}K\pi$ Dalitz-plot model.

Intermediate state	Fit fraction	Phase (°)
$DK^{*0}(892)$	0.46	0
$DK_0^{*0}(1430)$	0.0001	284
$DK_2^{*0}(1430)$	0.12	221
$DK^{*0}(1680)$	0.02	128
$D_2^{*-}(2460)K^+$	0.34	325
$D_0^-(2400)K^+$	0.02	267
Nonresonant $DK\pi$	0.06	140

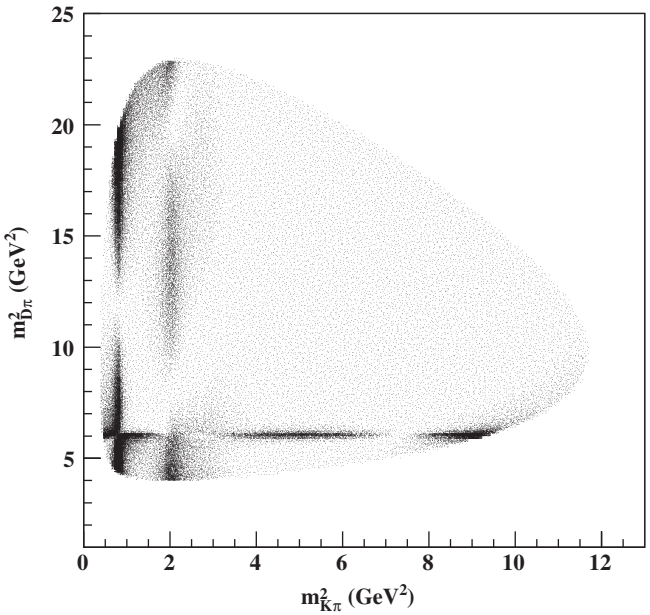

FIG. 4. High-statistics $B \to D_{\rm fav}K\pi$ Dalitz-plot distribution generated with our nominal model. Structures due to $DK^{*0}(892)$, $DK_2^{*0}(1430)$, and $D_2^{*-}(2460)K^+$, as well as the nonresonant contribution, are clearly apparent.

Table I summarizes the parameters of the resonances used in our analysis. Table II gives the fit fractions and relative phases of the various intermediate states that contribute to our $B \to DK\pi$ Dalitz-plot model. The parameters given are appropriate for the case that the neutral D meson decays to a favored, quasi-flavor-specific final state (namely, $B^0 \to DK^+\pi^-$, $D \to K^+\pi^-$ and charge conjugate). An example Dalitz-plot distribution generated from this model is shown in Fig. 4.

We derive the Dalitz-plot distributions for other D-decay final states using the equations presented in Sec. II and initially taking $\gamma = 60°$. We consider several different possible values of r_B and δ_B for the $DK^{*0}(892)$ amplitudes, while for the less significant contributions from other DK^* channels we simply set $r_B = 0.4$ and $\delta_B = 0°$. We note that our nominal value of $r_B = 0.4$ is at the upper end of the experimentally allowed range for this parameter (e.g. the UTfit Collaboration gives $r_B(DK^{*0}(892)) \in [0.081, 0.397]$ at 95% confidence level [32]), but it is convenient to use this value to allow comparison with previous studies.

We use our Dalitz-plot model to generate ensembles of event samples corresponding to the different D meson final states. The numbers of events are based on expectations for one year of nominal luminosity at LHCb (2 fb^{-1}) [12], assuming that the efficiency does not vary across the Dalitz plot. The exact numbers in each sample vary as functions of the input values of the parameters (particularly δ_B and γ), but typically are around 7300 for $D_{\rm fav}K\pi$, 700 for $D_{\rm sup}K\pi$, and 600 for $D_+K\pi$ (for B^0 and $\bar{B}^0$ decays combined).

IV. RESULTS WITH THE QUASI-TWO-BODY APPROACH

We first study the sensitivity to γ in the quasi-two-body approach. We take the six Dalitz-plot distributions ($D_{\rm fav}K\pi$, $D_{\rm sup}K\pi$, and $D_+K\pi$ all for both $\bar{B}^0$ and B^0) generated as described in the previous section, and apply selection requirements to select the DK^* dominated region. We then perform χ^2 minimization to fit the yields in each sample to determine five parameters: γ, r_S, δ_S, κ and an overall normalization. The parameters r_D and δ_D are fixed to their measured values (0.0616 and $-158°$, respectively). For each pseudoexperiment we perform ten fits with initial values of the parameters randomized in the ranges $\gamma \in [0, 2\pi)$, $r_B \in [0, 1)$, $\delta_B \in [0, 2\pi)$, $\kappa \in [0, 1)$, and we take the results of the fit with the smallest χ^2.

The selection requirements for the K^* are an interesting subtopic worthy of some discussion. The width of the $K\pi$ invariant-mass window around the nominal K^* mass affects the size of the event samples. Increasing the width yields greater statistics so that one would naively expect a reduction in the statistical uncertainty on γ. Unfortunately, increasing the width of the $K\pi$ invariant-mass window also leads to an increase in the dilution from the non-DK^* component of the amplitude, i.e. a decrease in κ, which tends to decrease the sensitivity to γ. Hence, it is important to optimize the K^* selection requirements.

One can increase κ by introducing a $D_2^*(2460)$ veto (e.g. rejecting events that satisfy $|M_{D\pi} - M_{D_2^*}| < 75$ MeV). This veto has a rather minimal impact on the statistics. In our nominal model with $\delta_B = 180°$, choosing to use $|M_{K\pi} - M_{K^*(892)}| < 150$ MeV yields $\kappa = 0.93$. Applying the $D_2^*(2460)$ veto above increases this to $\kappa = 0.97$. Decreasing the $K\pi$ invariant-mass window to $|M_{K\pi} - M_{K^*(892)}| < 50$ MeV yields $\kappa = 0.99$; however, with the limited statistics in our pseudoexperiments, this decrease in dilution is counterbalanced by the loss of statistics. Experiments with higher statistics may benefit by using a tighter $K\pi$ invariant-mass window. In the results below, we proceed using the $D_2^*(2460)$ veto discussed above and requiring the $K\pi$ invariant mass to be within 150 MeV of the nominal K^* mass.

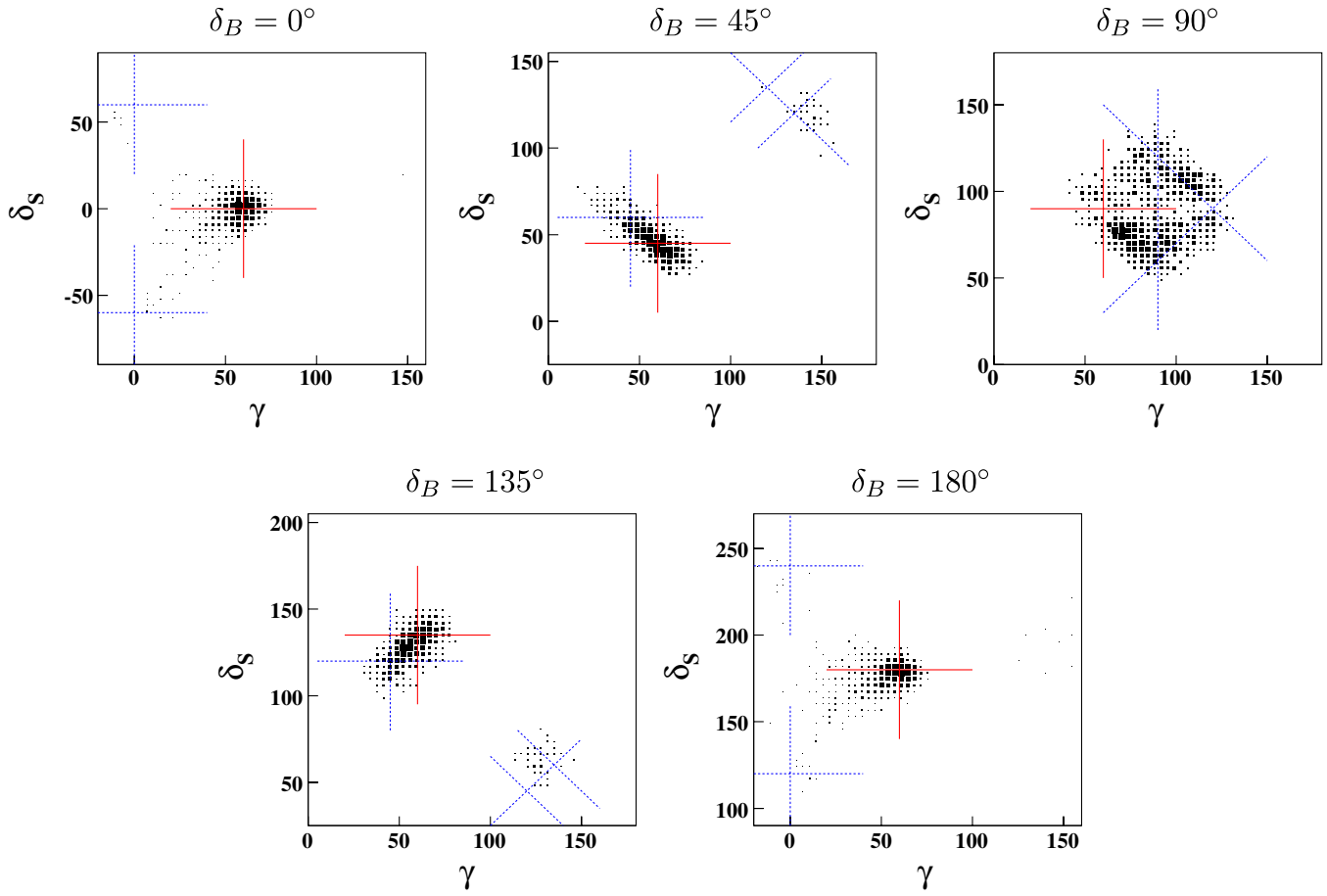

FIG. 5 (color online). Distributions of fitted values of γ in the quasi-two-body approach, with different input values of δ_B. These results are obtained with $\gamma = 60°$ and $r_B = 0.4$. The location of each of the generated solutions for $\kappa = 1$, i.e. $\delta_S = \delta_B$, is given by a red solid cross. The locations of each of the ambiguous solutions obtained for $\kappa = 1$ and $r_D = 0$ are given by the intersections of the blue dashed lines.

TABLE III. Results for γ obtained from the quasi-two-body analysis, with different input values of δ_B and a comparison with the results of Ref. [12]. These results are obtained with $\gamma = 60°$ and $r_B = 0.4$. See the text for details.

	γ (°)						
	κ free				κ locked		Ref. [12]
	Distribution		Gaussian fit		Gaussian fit		
	Mean	rms	μ	σ	μ	σ	σ
$\delta_B = 0°$	55.5	14.6	57.7	7.3	60.1	5.9	6.2
$\delta_B = 45°$	60.2	19.6	57.4	10.6	57.8	10.3	10.8
$\delta_B = 90°$	88.3	17.9					12.7
$\delta_B = 135°$	60.4	18.0	56.6	9.4	56.3	9.7	9.5
$\delta_B = 180°$	55.1	19.2	56.6	7.4	59.7	5.5	5.2

Results from the pseudoexperiments for various different input values of δ_B are shown in Fig. 5. It is apparent that there is a strong correlation between the fitted values of γ and δ_S, and moreover that there are ambiguities in the solution that are particularly pronounced for values of δ_B near 90°. The locations of each of the ambiguous solutions for the case where $r_D = 0$ are also shown in Fig. 5. The ambiguities in the solutions found by fitting our data are close to these values. Since r_D is small (our data were generated with $r_D = 0.0616$), statistical fluctuations can lead to the best χ^2 value being obtained near one of the ambiguous solutions. The inability to resolve such ambiguities is a limitation of the quasi-two-body method.

As a consequence of these ambiguities, the distributions of the fitted values of γ are not Gaussian. Therefore, in Table III, we report both the mean and rms of each distribution as well as the corresponding values obtained by fitting the data in the regions near the generated values of γ to Gaussian line shapes, i.e. ignoring the ambiguities in the solution. For $\delta_B = 90°$, it is not possible to separate the correct solutions from the ambiguous solution, so we have not performed a Gaussian fit to the distributions for this sample.

TABLE IV. Results for γ obtained from the quasi-two-body analysis, with different input values of r_B. These results are obtained with $\gamma = 60°$, $\delta_B = 0°$, and κ free.

	γ (°)			
	Distribution		Gaussian fit	
	Mean	rms	μ	σ
$r_B = 0.4$	55.5	14.6	57.7	7.3
$r_B = 0.3$	57.0	21.1	56.8	9.7
$r_B = 0.2$	58.9	29.3	56.9	11.8

We have also considered an alternative approach to the fits, in which the value of κ is fixed. Although κ can only be measured from analysis of $B \to DK\pi$ Dalitz plots (so that if this measurement can be performed, the Dalitz-plot analysis will most likely be feasible), it is conceivable that κ may be determined from theory, or from a different experiment. We therefore repeat the fits with κ constrained to the values obtained directly from our model. This approach leads to an improvement in the resolution on γ near some solutions (e.g., near the true solution for $\delta_B = 0°$), but does not remove the ambiguities (see Fig. 6). The results obtained by fitting the regions near the generated values of γ to Gaussian line shapes can be found in Table III. This provides a comparison with Ref. [12], where the same approach was used to estimate the sensitivity to γ using the quasi-two-body approach on one nominal year's data from LHCb. Despite several important differences between our toy study and the detailed sensitivity study of Ref. [12], the results are in very good agreement (see Table III). This provides confidence in the absolute scale of our sensitivity estimates.

The results obtained by varying r_B in our model are given in Table IV. As is well known, the sensitivity to γ reduces as r_B becomes smaller. It is also clear that the effect of ambiguities becomes more significant, since the discrepancy between the rms of the whole distributions and the width of the Gaussian peak near the correct solution increases.

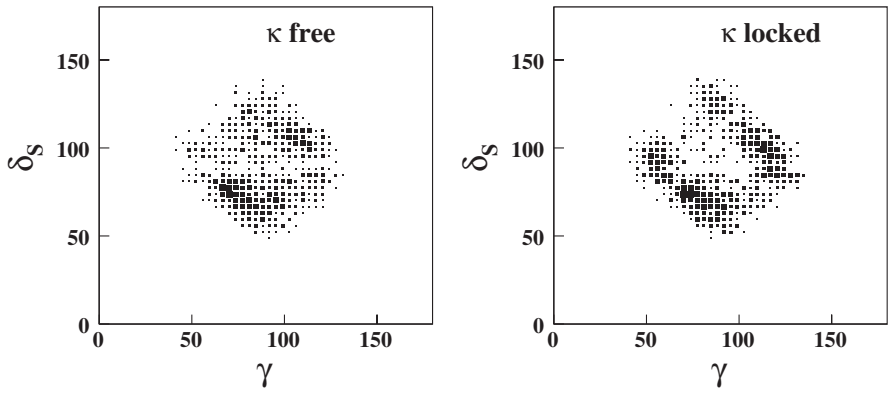

FIG. 6. Distributions of fitted values of γ in the quasi-two-body approach with κ free (left) and fixed (right). These results are obtained with $\gamma = 60°$, $\delta_B = 90°$, and $r_B = 0.4$.

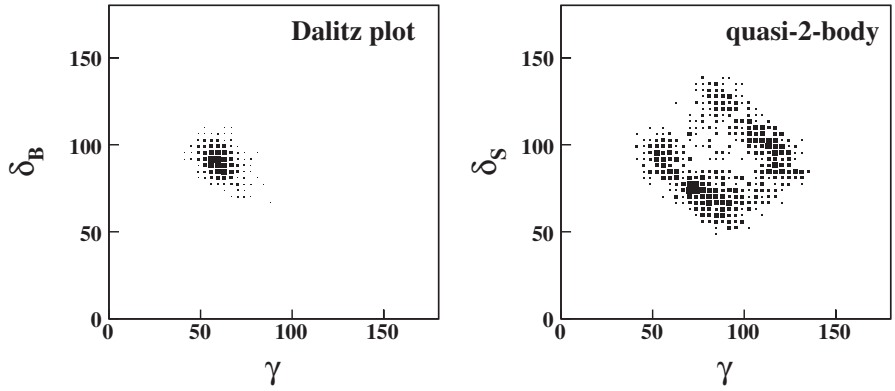

FIG. 7. Distributions of fitted values of γ in the amplitude (left) and quasi-two-body (right) approaches. These results are obtained with $\gamma = 60°$, $\delta_B = 90°$, and $r_B = 0.4$.

V. RESULTS WITH THE AMPLITUDE ANALYSIS

To study the sensitivity to γ using the Dalitz-plot analysis, we perform a simultaneous maximum likelihood fit to all six Dalitz-plot distributions. We initially fix r_D and δ_D to their measured values, leaving 24 free parameters (γ, four parameters—Δ, ϱ, r_B and δ_B—for each K^*-type resonance and nonresonant contribution, and two—magnitude and phase—for each D^*-type resonance, with one phase fixed). As before, for each pseudoexperiment we perform multiple fits with randomized initial parameter values, and we take the results of the fit with the smallest negative log likelihood.

In Sec. IV, we found that the quasi-two-body approach was, in many cases, unable to resolve ambiguities in the solution. This was especially true for values of δ_B near 90°. Figure 7 shows the distributions of results from the pseudoexperiments generated with $\delta_B = 90°$ for the amplitude and quasi-two-body approaches. The additional information utilized in the amplitude analysis is sufficient to remove the ambiguities in the solution.

The distributions of the fit results for the parameters $r_B(DK^*(892))$, $\delta_B(DK^*(892))$, and γ obtained from the pseudoexperiments generated with $\delta_B = 0°$ are shown in Fig. 8. We fit the distributions with Gaussian line shapes, since all are consistent with this shape (this is true for all δ_B values), and report the means and widths in Table V. The resolution on γ varies between 4.2°–5.8°, depending on the value of δ_B, in our nominal model. Thus, unlike for the quasi-two-body approach (Table III), the sensitivity to γ is not strongly dependent on the value of δ_B.

The physical values of r_B and γ may be different from those used in our model. To study how this would affect our results, we vary the values of r_B and γ in our model and fit the data using the same procedure outlined above. The results obtained considering $0.2 \leq r_B \leq 0.4$ are given in Table VI. As expected, the sensitivity to γ decreases as r_B decreases; however, even for $r_B = 0.2$ the distribution of fit results is still approximately Gaussian, and the resolution on γ is still 7°. The results obtained considering $45° \leq \gamma \leq 75°$ are given in Table VII. We conclude that the

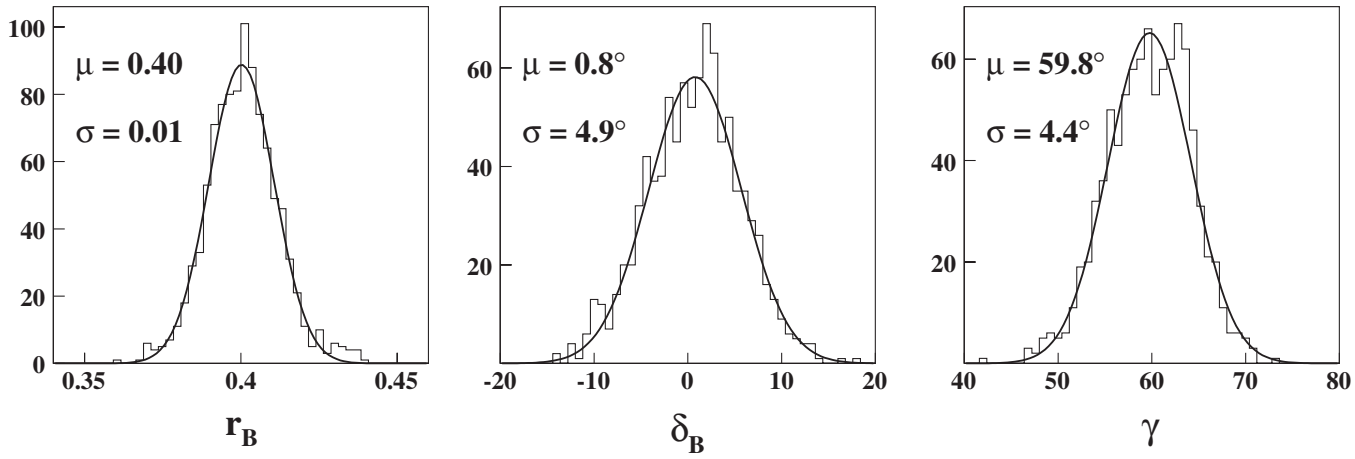

FIG. 8. Distributions of fitted values of r_B (left), δ_B (middle), and γ (right) in the amplitude analysis. These results are obtained with $\gamma = 60°$, $\delta_B = 0°$, and $r_B = 0.4$.

TABLE V. Results for $r_B(DK^*(892))$, $\delta_B(DK^*(892))$, and γ from the Dalitz-plot analysis, with different input values of δ_B. These results are obtained with $\gamma = 60°$ and $r_B = 0.4$.

	r_B		δ_B (°)		γ (°)	
	μ	σ	μ	σ	μ	σ
$\delta_B = 0°$	0.40	0.01	0.8	4.9	59.8	4.4
$\delta_B = 45°$	0.40	0.01	46.2	6.0	59.2	5.5
$\delta_B = 90°$	0.40	0.01	90.2	6.4	59.8	5.7
$\delta_B = 135°$	0.40	0.01	134.0	6.3	59.3	5.8
$\delta_B = 180°$	0.40	0.01	179.8	4.2	59.7	4.2

TABLE VI. Results for $r_B(DK^*(892))$, $\delta_B(DK^*(892))$, and γ from the Dalitz-plot analysis, with different input values of r_B. These results are obtained with $\gamma = 60°$ and $\delta_B = 0°$.

	r_B		δ_B (°)		γ (°)	
	μ	σ	μ	σ	μ	σ
$r_B = 0.4$	0.40	0.01	0.8	4.9	59.8	4.4
$r_B = 0.3$	0.30	0.01	0.7	5.9	60.0	5.3
$r_B = 0.2$	0.20	0.01	0.6	7.0	59.5	7.0

TABLE VII. Results for $r_B(DK^*(892))$, $\delta_B(DK^*(892))$, and γ from the Dalitz-plot analysis, with different input values of γ. These results are obtained with $r_B = 0.4$ and $\delta_B = 0°$.

	r_B		δ_B (°)		γ (°)	
	μ	σ	μ	σ	μ	σ
$\gamma = 45°$	0.40	0.01	1.2	6.0	44.6	5.2
$\gamma = 60°$	0.40	0.01	0.8	4.9	59.8	4.4
$\gamma = 75°$	0.40	0.01	0.4	4.5	74.8	4.0

TABLE VIII. Results for $r_B(DK^*(892))$, $\delta_B(DK^*(892))$, and γ from the Dalitz-plot analysis, with different input values of $\Delta[DK^{*0}(892)]$. These results are obtained with $r_B = 0.4$, $\delta_B = 0°$, and $\gamma = 60°$.

$\Delta[DK^{*0}(892)]$	r_B		δ_B (°)		γ (°)	
	μ	σ	μ	σ	μ	σ
55°	0.40	0.01	0.5	4.9	59.7	4.1
145°	0.40	0.01	0.4	4.9	59.7	4.3
235°	0.40	0.01	0.0	5.0	59.5	4.0
325°	0.40	0.01	0.8	4.9	59.8	4.4

sensitivity to γ does not depend strongly on the value of γ itself.

There are a number of parameters in our model which are not well constrained by data; however, most of these are not expected to impact significantly the sensitivity to γ. For example, the strong phase between the $D_2^{*-}(2460)K^+$ and $\bar{D}K^{*0}(892)$ amplitudes, which we denote by $\Delta[DK^{*0}(892)]$, could be very different from the value used in our model. To determine what effect the value of this parameter has on the extracted value of γ, we vary $\Delta[DK^{*0}(892)]$ in our model over the physically allowed range, $[0, 2\pi)$, and refit the data. The fit results, given in Table VIII, show that the impact on the sensitivity to γ is minimal.

TABLE IX. Results for $r_B(DK^*(892))$, $\delta_B(DK^*(892))$, and γ from the Dalitz-plot analysis, with $r_B(DK_0^{*0}(1430)) = 0$, $r_B(DK_2^{*0}(1430)) = 0$, and $r_B(DK^{*0}(1680)) = 0$. These results are obtained with $r_B = 0.4$, $\delta_B = 0°$, and $\gamma = 60°$.

r_B		δ_B (°)		γ (°)	
μ	σ	μ	σ	μ	σ
0.40	0.01	0.1	5.2	59.0	5.6

None of the parameters for the $DK_0^{*0}(1430)$, $DK_2^{*0}(1430)$, or $DK^{*0}(1680)$ amplitudes is well constrained by data. To see what effect the presence of CP violation in these amplitudes has on the sensitivity to γ, we set $r_B(DK_0^{*0}(1430)) = 0$, $r_B(DK_2^{*0}(1430)) = 0$, and $r_B(DK^{*0}(1680)) = 0$ in our model and refit the data. The results obtained for this model variation are given in Table IX. There is no appreciable bias on the extracted value of γ, and the resolution on γ decreases by only 1.2°. This is not surprising given the relatively small contributions to the total $B \to DK\pi$ amplitude from $DK_0^{*0}(1430)$, $DK_2^{*0}(1430)$, and $DK^{*0}(1680)$ (see Table II). If, however, in real data these or any other DK^*-type amplitudes do contribute strongly to $B \to DK\pi$ (and have sufficiently large CP violation), then the sensitivity to γ could be better than that obtained from our nominal model. To further test how mismodeling of the Dalitz plot may affect the extracted value of γ, we refit the data from our nominal model using only the $DK^*(892)$, $D_2^-(2460)K$, and nonresonant amplitudes (fixing all others to zero). The results are shown in Table X. Again, there is little impact on the extracted values, indicating that this analysis may suffer much less model-related uncertainties than some other methods to extract γ [22,23].

We have also tested how the addition of D_s-type resonances may affect the analysis. We add to the model a contribution from $D_{s1}^*(2700)$, the magnitude of which is based on the assumption

$$\frac{\mathcal{B}(B \to D_{sJ}\pi)}{\mathcal{B}(B \to D_{sJ}D)} \approx \frac{\mathcal{B}(B \to D_s^{(*)}\pi)}{\mathcal{B}(B \to D_s^{(*)}D)}. \tag{13}$$

TABLE X. Results for $r_B(DK^*(892))$, $\delta_B(DK^*(892))$, and γ from the Dalitz-plot analysis, where the fit model contains only the $DK^*(892)$, $D_2^-(2460)K$, and nonresonant amplitudes. These results are obtained with $r_B = 0.4$, $\delta_B = 0°$, and $\gamma = 60°$.

r_B		δ_B (°)		γ (°)	
μ	σ	μ	σ	μ	σ
0.40	0.01	−1.0	4.4	60.2	4.5

TABLE XI. Results for $r_B(DK^*(892))$, $\delta_B(DK^*(892))$, and γ obtained from the Dalitz-plot analysis, where the $D^*_{s1}(2700)$ has been added to our nominal model. These results are for $r_B = 0.4$, $\delta_B = 0°$, and $\gamma = 60°$.

r_B		δ_B (°)		γ (°)	
μ	σ	μ	σ	μ	σ
0.40	0.01	0.8	5.0	59.9	4.3

The right-hand side of this expression is found to be $(2.4 \pm 0.6) \times 10^{-3}$ for D_s and $(3.3 \pm 0.9) \times 10^{-3}$ for D^*_s [31]. Using results from Ref. [30], we estimate

$$\mathcal{B}(B \to D^*_{s1}(2700)\pi) \times \mathcal{B}(D^*_{s1}(2700) \to DK) \approx 2.7 \times 10^{-3} \times 11.3 \times 10^{-4} \approx 3 \times 10^{-6}. \quad (14)$$

We add a contribution from this amplitude, with an arbitrary phase, to the model described in Table II. The results of fits to pseudoexperiments generated with this modified model are summarized in Table XI. There is little or no improvement in the sensitivity to γ compared to the nominal model. This can be understood since the corner of the Dalitz plot where the $D^*_{s1}(2700)$ and $K^*(892)$ would interfere is excluded by kinematic constraints (see Fig. 4). Following this reasoning, larger effects from D_{sJ}-type resonances would be possible if there were significant contributions to the Dalitz plot from heavier K^* and/or heavier D_{sJ} resonances.

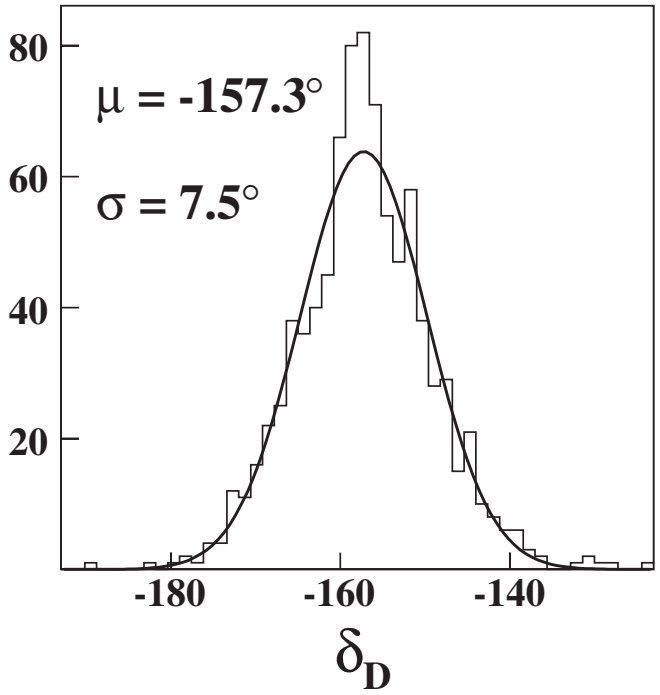

FIG. 9. Distribution of fitted results for δ_D obtained in the amplitude analysis when fitting with δ_D as a free parameter. The mean and width obtained by fitting the distribution to a Gaussian line shape (solid line) are shown on the plot. The generated value of δ_D is $-158°$.

In our nominal fit, we fix the values of δ_D and r_D. However, the value of δ_D is currently not precisely measured: $\delta_D = (-158 \pm 11)°$ [18,19,33]. To study what effect this parameter can have on our results, we rerun the fits described above (on our nominal model) starting the value of δ_D randomly in the range $[0, 2\pi)$. The results obtained for δ_D are shown in Fig. 9. The resolution extracted for δ_D is 7.5°, which is less than the uncertainty on current measurements. Fitting with δ_D free has no significant effect on our results for $r_B(DK^*(892))$, $\delta_B(DK^*(892))$, and γ (for all model values of δ_B).

VI. EXPERIMENTAL EFFECTS

The study reported in the previous section neglected a number of experimental effects which will surely impact the sensitivity to γ in any real-world experiment. The effect most likely to have the largest impact on the resolution is the presence of background events. To study how this might affect the sensitivity to γ, we generate background events by sampling from a flat Dalitz distribution. For real data, there will almost certainly be some features present in the shape of the background; however, for our purposes, a flat background model should be sufficient. We take the expected background yields in each of the six final states to be equivalent. This should be a reasonable approximation provided the main source of background events is from combinatorics (a plausible assumption for LHCb). The ratio of background to signal, B/S, is defined here as the ratio of the number of expected background events to the number of expected signal events for the final state with the smallest expected signal yield. We generate background events according to this prescription for the ratios $B/S = 1$, 2, 10, 50, and 100, and fit the data using the same procedure as in the previous section.

For $B/S \gtrsim 10$, ambiguities in the solution begin to appear (see Fig. 10), just as they did using the quasi-two-body approach without background. About 2% of pseudoexperiments with $B/S = 10$ find their best likelihood in an ambiguous solution. This number steadily increases as the background increases, reaching about 25% for $B/S = 100$. This can be understood since, as the background increases, it becomes more difficult to extract cleanly the amplitudes with smaller contributions. The amplitude with the strongest contribution in our model is $DK^*(892)$. Thus, in the presence of a large background contamination, the amplitude analysis essentially reduces to the quasi-two-body approach. This results in the ambiguities in the solution found in the quasi-two-body approach (without background) appearing in the amplitude analysis if the background yields are large.

Our studies show that the background level should be kept to $B/S \lesssim 20$ in order to take full advantage of the benefits of the amplitude analysis. This appears achievable,

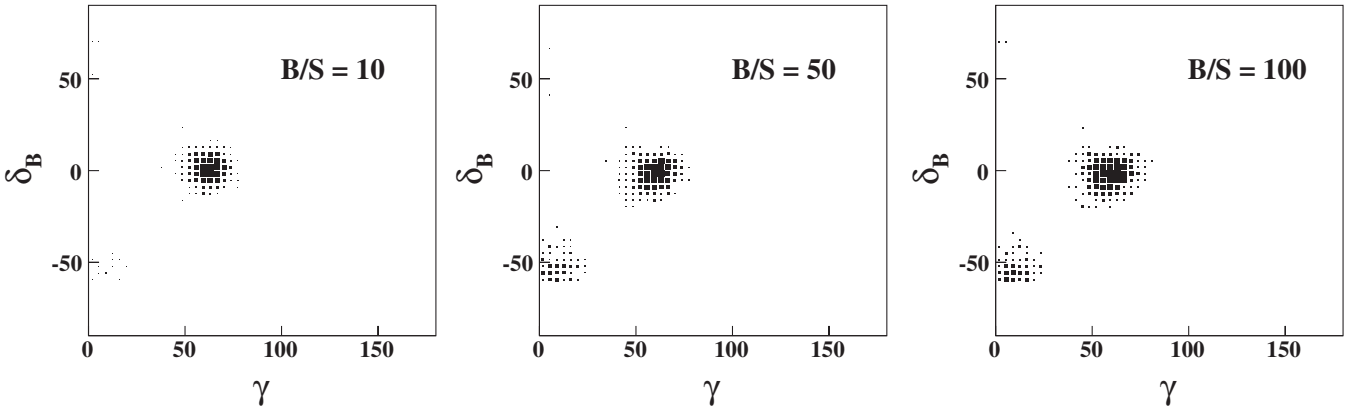

FIG. 10. Distributions of fitted values of γ in the Dalitz-plot approach, for $B/S = 10$, 50, 100. These results are obtained with $\gamma = 60°$, $\delta_B = 0°$, and $r_B = 0.4$.

even in a hadronic environment. For $B/S = 20$ the ambiguities in the solution still appear at the few percent level; however, one can study the likelihood contours to determine whether the solution for any given experiment may have ambiguities. The results obtained from an experiment with such a background would need to take this into account. Note also that these results are for a data sample roughly equivalent to one nominal year's data taking at LHCb, and that effects due to ambiguities would be expected to be ameliorated with larger data samples.

The results obtained for $r_B(DK^*(892))$, $\delta_B(DK^*(892))$, and γ are given in Table XII. The ambiguities in the solution discussed above have been ignored in these results, i.e. the means and widths for $B/S \geq 10$ are obtained by fitting the region around the true solution to a Gaussian line shape. The effects of the background on the resolution are minimal. The resolution of γ for $B/S = 10$ is only 1° worse than with no background. Even for $B/S = 100$ the resolution is only about 60% worse. Thus, the most important impact of the presence of background events is their ability to lessen the power the amplitude analysis has to break the ambiguities found in the quasi-two-body analysis.

One particularly dangerous form of background can arise from particle misidentification. Usually, if a pion is misidentified as a kaon, or vice versa, there is a resulting shift in any reconstructed invariant mass, allowing these backgrounds to be identified and rejected. However, in the $B^0 \to DK^+\pi^-$ decay there is a possibility of double misidentification with the π^- being misreconstructed as a K^- simultaneously with the K^+ being misreconstructed as a π^+. In this case the invariant-mass shifts would largely cancel, and the main difference from the distribution for correctly reconstructed signal events would be a significant broadening of the resolution. Such effects are expected to be extremely rare, but since they would result in a distortion of the Dalitz plot and an incorrect flavor assignment they will require careful study in the experimental analysis. Similar double misidentification effects can arise in the reconstruction of $D \to K\pi$. These have been studied in the context of analyses of $B^\pm \to DK^\pm$ with $D \to K^\pm\pi^\mp$ [34] and charm mixing [35] at LHCb where it has been found that a combination of appropriate particle identification requirements and a veto on the invariant mass calculated with the mass assignments reversed provides an effective way to remove the background with only small loss of signal efficiency.

Another experimental effect which must be taken into account in a real experimental analysis is the variation of reconstruction efficiency across the Dalitz plot. Our study has assumed that the efficiency is flat, but in reality one would expect the probability to reconstruct successfully a decay to be lower at the edges of phase space near the corners of the Dalitz plot. If the shape of the efficiency function is known, this can be taken into account in the analysis. However, systematic effects arise since the efficiency is typically measured using Monte Carlo simulations, which inevitably will not give exactly the same behavior as the data.

It is impossible to give a quantitative estimate of how large an effect this may be. Nonetheless, there is a strong qualitative reason to believe that it will not be a major problem. The key point is that the our amplitude analysis extracts γ from the difference between $DK\pi$ Dalitz-plot

TABLE XII. Results for $r_B(DK^*(892))$, $\delta_B(DK^*(892))$, and γ obtained from the Dalitz-plot analysis, with different levels of background. These results are for $r_B = 0.4$, $\delta_B = 0°$, and $\gamma = 60°$.

	r_B		δ_B (°)		γ (°)	
	μ	σ	μ	σ	μ	σ
$B/S = 0$	0.40	0.01	0.8	4.9	59.8	4.4
$B/S = 1$	0.40	0.01	0.1	5.1	59.8	4.9
$B/S = 2$	0.39	0.01	−0.8	5.2	61.0	5.0
$B/S = 10$	0.40	0.01	1.2	5.2	62.1	5.4
$B/S = 50$	0.40	0.01	−1.5	5.8	59.5	6.2
$B/S = 100$	0.39	0.01	−1.9	6.0	58.8	7.2

distributions with the D meson reconstructed in different decay modes ($D \to K\pi$ and $D \to CP$ eigenstates). Data/MC differences can be expected to cancel in the ratio of Dalitz-plot distributions, unless there is a momentum dependence in the ratio of efficiencies to reconstruct the D meson in the different final states. Such an effect should be possible to study using control samples.

VII. SUMMARY

We have presented a feasibility study of an extension to the recently proposed method to extract the unitarity triangle angle γ from amplitude analysis of $B \to DK\pi$ Dalitz plots. The analysis includes the cases where the neutral D meson is reconstructed in CP-even eigenstates as well as in CKM-favored and CKM-suppressed hadronic decays. Compared to the previously proposed quasi-two-body analysis, the amplitude analysis provides (i) at least 50% better sensitivity to γ, (ii) resolution of ambiguous solutions, (iii) much reduced dependence of the sensitivity on the strong phase δ_B, and (iv) the possibility to determine the poorly known parameter δ_D. The analysis appears to be relatively robust against mismodeling of the Dalitz plot, and performs well even when relatively large backgrounds are present. We conclude that this method appears to be a highly attractive addition to the family of methods that can be used to determine γ.

ACKNOWLEDGMENTS

We are grateful to our colleagues from the LHCb experiment, and would particularly like to thank Ignacio Bediaga, Alex Bondar, Ulrik Egede, Patrick Koppenburg, Anton Poluektov, and Guy Wilkinson for discussions. This work is supported by the Science and Technology Facilities Council (United Kingdom).

[1] N. Cabibbo, Phys. Rev. Lett. **10**, 531 (1963).
[2] M. Kobayashi and T. Maskawa, Prog. Theor. Phys. **49**, 652 (1973).
[3] M. Artuso *et al.*, Eur. Phys. J. C **57**, 309 (2008).
[4] T. E. Browder, T. Gershon, D. Pirjol, A. Soni, and J. Zupan, arXiv:0802.3201 [Rev. Mod. Phys. (to be published)].
[5] M. Antonelli *et al.*, arXiv:0907.5386.
[6] M. Gronau and D. London, Phys. Lett. B **253**, 483 (1991).
[7] M. Gronau and D. Wyler, Phys. Lett. B **265**, 172 (1991).
[8] D. Atwood, I. Dunietz, and A. Soni, Phys. Rev. Lett. **78**, 3257 (1997).
[9] D. Atwood, I. Dunietz, and A. Soni, Phys. Rev. D **63**, 036005 (2001).
[10] I. Dunietz, Phys. Lett. B **270**, 75 (1991).
[11] K. Akiba and M. Gandelman, Report No. CERN-LHCB-2007-050.
[12] K. Akiba *et al.*, Report No. CERN-LHCB-2008-031.
[13] J. Nardulli and S. Ricciardi, Report No. CERN-LHCb-2008-038.
[14] M. Gronau, Phys. Lett. B **557**, 198 (2003).
[15] S. Pruvot, M. H. Schune, V. Sordini, and A. Stocchi, arXiv:hep-ph/0703292.
[16] I. Bediaga (unpublished).
[17] T. Gershon, Phys. Rev. D **79**, 051301 (2009).
[18] J. L. Rosner *et al.* (CLEO Collaboration), Phys. Rev. Lett. **100**, 221801 (2008).
[19] D. M. Asner *et al.* (CLEO Collaboration), Phys. Rev. D **78**, 012001 (2008).
[20] M. Patel, Report No. CERN-LHCb-2009-011.
[21] A. Soffer, Phys. Rev. D **60**, 054032 (1999).
[22] A. Poluektov *et al.* (Belle Collaboration), Phys. Rev. D **73**, 112009 (2006).
[23] B. Aubert *et al.* (BABAR Collaboration), Phys. Rev. D **78**, 034023 (2008).
[24] J. Blatt and V. E. Weisskopf, *Theoretical Nuclear Physics* (Wiley, New York, 1952).
[25] C. Zemach, Phys. Rev. **133**, B1201 (1964).
[26] C. Zemach, Phys. Rev. **140**, B97 (1965).
[27] M. Williams, Comput. Phys. Commun. **180**, 1847 (2009).
[28] B. Aubert *et al.* (BABAR Collaboration), Phys. Rev. Lett. **96**, 011803 (2006).
[29] B. Aubert *et al.* (BABAR Collaboration), Phys. Rev. D **77**, 071102 (2008).
[30] J. Brodzicka *et al.* (Belle Collaboration), Phys. Rev. Lett. **100**, 092001 (2008).
[31] C. Amsler *et al.* (Particle Data Group), Phys. Lett. B **667**, 1 (2008).
[32] M. Bona *et al.* (UTfit Collaboration), J. High Energy Phys. 10 (2006) 081.
[33] E. Barberio *et al.* (Heavy Flavor Averaging Group), arXiv:0808.1297.
[34] M. Patel, Report No. CERN-LHCB-2006-066.
[35] P. M. Spradlin, G. Wilkinson, and F. Xing, Report No. CERN-LHCB-2007-049.